Theoretical Comparison of Ketene Dimerization in the Gas and Liquid Phase

Giovanni Morales,[†] Ramiro Martínez,[†] and Tom Ziegler*[,‡]

Department of Chemistry, University of Calgary, 2500 University Drive, Calgary, Alberta, Canada T2N 1N4, and Escuela de Ingeníería Química, Universidad Industrial de Santander, Bucaramanga, Colombia

Received: November 26, 2007; In Final Form: January 8, 2008

We present the first theoretical comparison between ketene dimerization in gas phase and ketene dimerization in solution. Density functional theory (DFT) calculations on the ketene dimerization were carried out considering the following product dimers: diketene (d-I), 1,3-cyclobutanedione (d-II), 2,4-dimethylene-1,3-dioxetane (d-III), and 2-methyleneoxetan-3-one (d-IV). All structures were optimized at the PW86x+PBEc/DZP level of theory. Based on these geometries, a total of 58 meta and hybrid functionals were used to evaluate the heat of dimerization. The MPW1K functional was found to fit the experimental data best and subsequently used in the final analyses for all energy calculations. It was found on both kinetic and thermodynamic grounds that only d-I and d-II are formed during ketene dimerization in gas phase and solution. In gas phase, d-I is favored over d-II by 2 kcal/mol. However, the dimerization barrier for d-I is 1 kcal/mol higher than for d-II. Solvation makes dimerization more favorable. On the enthalpic surface this is due to a favorable interaction between the dimer dipole moment and solvent molecules. The dimer is stabilized further on the Gibbs energy surface by an increase of the dimerization entropy in solution compared to gas phase. The species d-I remains the most stable dimer in solution by 1 kcal/mol. Kinetically, the dimerization barriers for the relevant species d-I and d-II are cut in half by solvation, due to both favorable dimer−dipole/solvent interactions ($\Delta H^{\ddagger}$, $\Delta G^{\ddagger}$) and an increase in the activation entropies ($\Delta S^{\ddagger}$). While the dimerization barrier for d-II is lowest for the gas phase and toluene, the barrier for d-I formation becomes lowest for the more polar solvent acetone by 1 kcal/mol as d-I dimerization has the most polar transition state.

Introduction

Ketenes are heterocumulene compounds having one oxygen atom in a cumulative arrangement[1] (RR′C═C═O). Since their discovery, ketenes have been recognized as important precursors for other species and they have been the subject of numerous investigations. Ketenes are of major importance as starting materials in organic synthesis, for example, in the formation of β-lactams leading to penicillins by a [2+2] cycloadditions with imines,[1,2a−c] the formation of prostaglandin precursors,[2c−d] the syntheses of benzoquinones,[2e] the enantioselective synthesis of allenes,[2f] the synthesis of α-amino acid derivatives,[2g] and the production of ketene heterodimers for the synthesis of proteasome inhibitors.[2h] The reaction of ketene (we refer to the parent ketene, $H_2C{=}C{=}O$, from this point onward unless otherwise stated) with itself was described almost simultaneously in 1908 by Chick and Wilsmore[3a] in England and by Staudinger and Klever[3b] in Germany. Among the products that conceivably could be formed during the ketene dimerization are diketene (d-I), 1,3-cyclobutanedione (d-II), 2,4-dimethylene-1,3-dioxetane (d-III), and 2-methyleneoxetan-3-one (d-IV). The structures of these products are shown in Chart 1. The highly reactive diketene (d-I), which is prepared on a multimillion pound per year scale by the pyrolysis of acetic acid, is an industrially important raw material used in the preparation of acetoacetates and acetoacetamides.[4,5] The diketene is also used for introducing functionalized C2, C3, and C4 units into organic compounds.[2c] It is, in addition, a potent bactericide useful for disinfecting large areas.[5] 1,3-Cyclobutanedione (d-II) is utilized in the production of squaric acid, which is an intermediate reagent for the production of pharmaceuticals, dyes and herbicides.[6] The 1,3-cyclobutanedione ring was recently incorporated into a novel copolymer prepared by cycloaddition polymerization of the bisketene derived from 1,4-cyclohexanedicarbonyl chloride.[7] Polymers that contain the 1,3-dioxetane (d-III) can be used as constituents in electrophotographic photoreceptors[8a] and oil-based inks[8b] in the photographic and lithographic industries, respectively. The oxetan-3-one structure (d-IV) has been found in numerous steroids whose biological functions include anti-inflammatory activity and anti-glucocorticoid activity, while some of them act as oral diuretics.[9]

It is well-known that ketene can undergo dimerization in polar solvents within a wide range of temperatures.[10,11] For the parent ketene the main product is diketene (d-I), whereas substituted ketenes afford cyclobutanediones (d-II-like structure). The activation enthalpy for ketene dimerization in acetone is determined experimentally to be 10 kcal/mol at room temperature.[10] Ketene dimerization in the gas phase is by contrast a slow process with an activation enthalpy of 31 kcal/mol,[12] and the major product is d-I. It is not established whether d-I is the major product as a result of kinetic or thermodynamic control or both. There have been several theoretical studies[13−17] of ketene dimerization in gas phase, starting with the work of Jug et al.[13] A recent investigation by Rode and Dobrowolski[17] finds from multilevel G3 calculations that d-I is more stable than d-II. The same authors also found the dimerization barrier to be higher for d-I than for d-II.

* To whom correspondence should be addressed: phone (403) 220-5368; fax (403) 289-9488; e-mail ziegler@ucalgary.ca.
[†] Universidad Industrial de Santander.
[‡] University of Calgary.

10.1021/jp711204v CCC: $40.75
Published on Web 03/12/2008

TABLE 1: Experimental Data Used in Equations 1−3

	MW,[a]	ρ,[a] g/mL	S^0_{liq},[a] J/(mol·K)	S^0_{gas}, J/(mol·K)	α[b]	$R \ln [V_{m,liq}/V_{m,gas}]$, cal/(mol·K)
acetone	58.10	0.7845	199.80	250.27[a]	0.20	−11.53
toluene	92.14	0.8668	220.96	340.00[c]	0.35	−10.81

[a] Reference 32. [b] See eq 1. [c] Reference 33.

CHART 1: Schematic Structures for the Four Ketene Dimers Studied in This Work

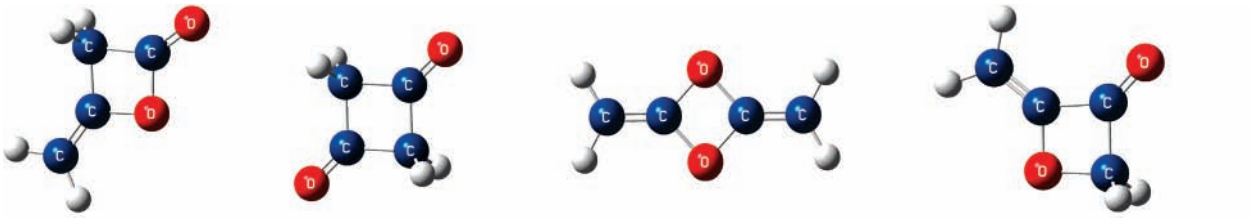

d-I Diketene | d-II 1,3-Cyclobutanedione | d-III 2,4-dimethylene-1,3-Dioxetane | d-IV 2-methyleneoxetan-3-one

It is surprising that there only are a few experimental and no theoretical investigations on ketene dimerization in condensed phase, even though the important industrial production of d-I by dimerization is possible only at ambient temperatures in the condensed phase.[10,12] The two experimental studies on the dimerization in condensed phase focus on the parent ketene[10] and dimethylketene,[19] respectively. In both investigations the rate of the reaction was second-order in ketene and increased with the polarity of the solvent. Moreover, it was found that the dimerization is an uncatalyzed process.[10,20] However, it is remarkable that the formation of the parent d-I dimer in the gas phase has a very high activation energy[12] (31 kcal mol^{-1}), whereas the activation energy is reduced to 10 kcal mol^{-1} in acetone.[10] We shall in the following examine how solvation effects modify the energetics of ketene dimerization as well as the structure of the species involved.

Computational Details

Geometry optimizations and frequency calculations were carried out using the exchange functional of Perdew−Wang (PW86x)[21] and the correlation functional of Perdew−Burke−Ernzerhof (PBEc).[22] A standard double-ζ Slater-type orbital (STO) basis with one polarization function was applied. The 1s electrons of C and O were treated within the frozen core approximation.[23] An auxiliary basis set of s, p, d, f, and g STOs was utilized to fit the molecular densities in order to represent the Coulomb and exchange potentials accurately in each self-consistent field (SCF) cycle.[24] Gas-phase electronic enthalpies were calculated from Kohn−Sham energies, and standard expressions[25] were used to calculate the remaining gas-phase enthalpic and entropic contributions at nonzero temperatures as well as zero-point energy (ZPE) corrections. Linear transit searches were carried out to locate transition states leading to each of the dimers as product. The intrinsic reaction coordinate (IRC)[26] method was applied to verify the TS structures for each dimer. Single-point energy calculations were carried out with different functionals based on the structures optimized with the PW86x+PBEc functional to test the sensitivity of the calculated energies against the choice of functionals. The calculations were carried out by use of the Amsterdam Density Functional (ADF) program package[27] versions 2004.02 and 2005.02.

Solvation enthalpies in acetone and toluene were obtained by employing the COSMO method[28] as implemented in ADF.[29] The solvent-excluding surface was constructed from the atomic radii of 1.16, 1.3, and 2.2 Å for H, O, and C, respectively. Values for the dielectric constant of 20.56 and 2.4 were used in the calculations for acetone and toluene, respectively. The solvation enthalpy was calculated as the difference between the gas-phase energy and the total energy calculated by use of the COSMO solvation model.

The method of Wertz[30] was employed for the calculation of solvation entropies in acetone and toluene. In the first step based on this method, the ideal-gas solute is compressed from standard conditions ($V_{m,gas}$) to the standard volume of the solvent ($V_{m,liq}$). Then the solute is transferred to the solvent, forming a hypothetical solution that has the intermolecular interactions of a dilute solution. In this step the solute loses a fraction of its remaining entropy. This fraction can be calculated by use of eq 1,[31] in which the numerator represents the change in entropy in the process of transfer. In the third step, the solute is expanded to the density of the solution at experimental conditions[10] (acetone, 0.524 mol/L; toluene, 0.910 mol/L). The solvation entropy is thus obtained from the sum of the entropy changes accompanying each step. Using the data reported in Table 1, we are able to calculate the entropy (calories per mole per kelvin) of solvation for a given molecule A in acetone $\Delta S(A)^0_{sol(acetone)}$ and toluene $\Delta S(A)^0_{sol(toluene)}$:

$$\alpha = \frac{S^0_{liq} - [S^0_{gas} + R \ln (V_{m,liq}/V_{m,gas})]}{[S^0_{gas} + R \ln (V_{m,liq}/V_{m,gas})]} \quad (1)$$

$$\Delta S(A)^0_{sol(acetone)} = -11.53 - 0.20[S(A)^0_{gas} - 11.53] + 6.55 \quad (2)$$

$$\Delta S(A)^0_{sol(toluene)} = -10.81 - 0.35[S(A)^0_{gas} - 10.81] + 4.642 \quad (3)$$

Results and Discussion

Our optimized gas-phase geometries for the four dimers are given in Figure 1, where they are compared to estimates from other sources. Optimized transition-state structures for the four dimerization processes are shown in Figure 2 for the gas phase and in Figure 3 for the liquid phase. Stationary points for the different structures were characterized by frequency calculations. The complete list of all calculated dimer and transition-state geometries, moments of inertia, dipole moments, and frequencies are given in the Supporting Information.

Dimer Gas-Phase Geometries. In the dimerization of two ketenes, each monomer makes use of a set of (π_{CC}/π^*_{CC}) orbitals (Chart 2) on the C=C double bond and a (π_{CO}/π^*_{CO})

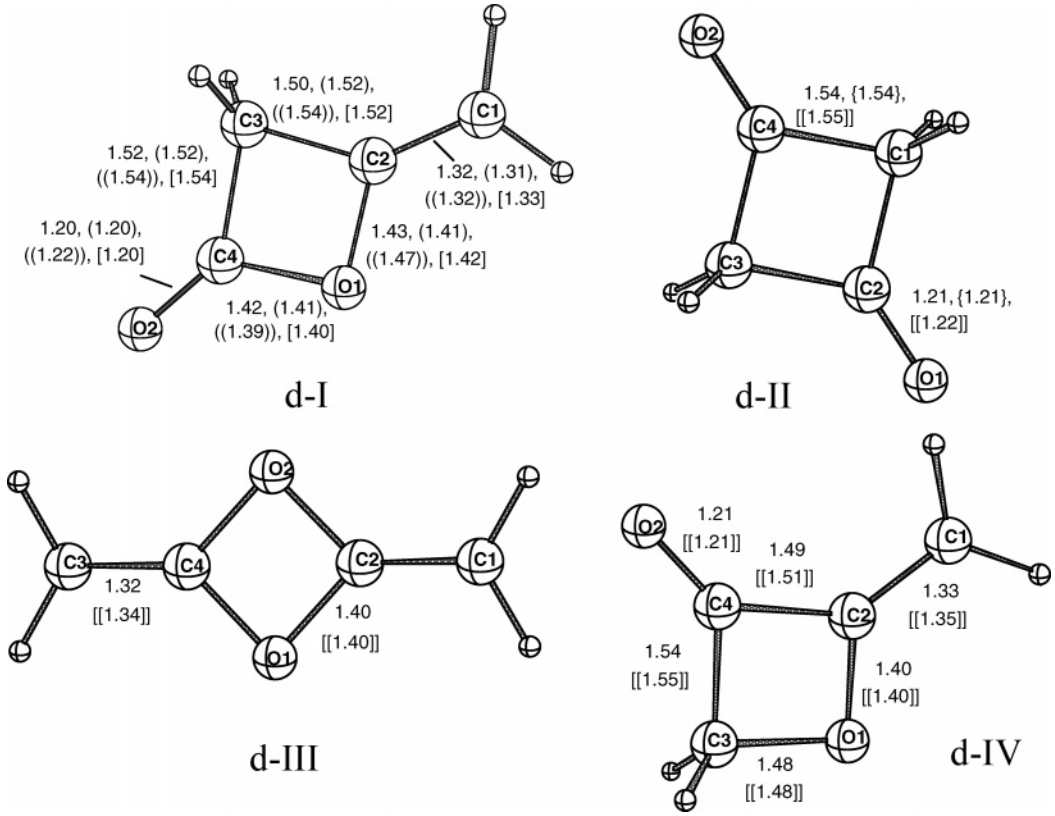

Figure 1. Bond lengths for the ketene dimers in gas phase (given in angstroms) from the current investigation compared to other estimates: electron diffraction,[35] in parentheses; X-ray structures,[36] in double parentheses; theoretical predictions of Seidl and Schaefer,[34] in brackets; theoretical predictions at the MP2/6-31G(d) level,[16] in braces; and theoretical predictions at the MP2/aug-cc-pVDZ level,[17] in double brackets.

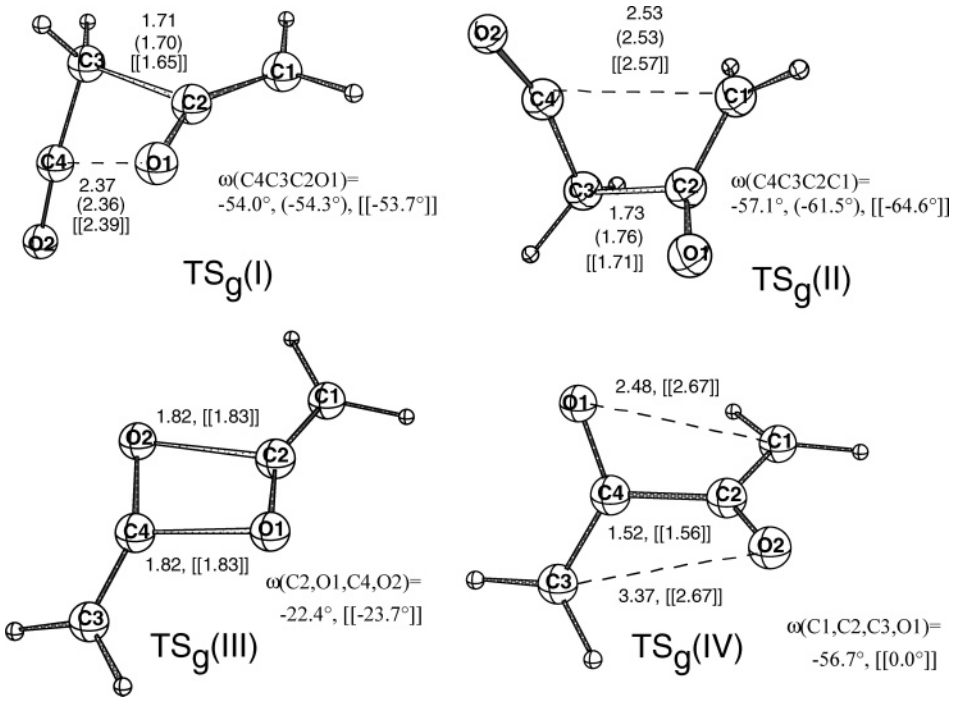

Figure 2. Some geometric parameters for ketene dimerization transition states in gas phase (bond lengths are given in angstroms): predictions at the MP2/6-31G(d) level,[16] in parentheses; predictions at the MP2/aug-cc-pVDZ level,[17] in double brackets.

set of orbitals (Chart 3) on the CO group. The two sets are perpendicular to each other. In d-I and d-IV, (π_{CC}/π^*_{CC}) on one monomer and (π_{CO}/π^*_{CO}) on the other are involved in the formation of the two new bonds during the dimerization process. In d-II, use is made of two (π_{CC}/π^*_{CC}) sets, whereas two (π_{CO}/π^*_{CO}) sets are involved in the bond formation for d-III; see Chart 1.

Our optimized molecular parameters for the d-I dimer are in good agreement with theoretical predictions at different levels of theory[16,17,34] (Figure 1). We obtain the same trends as in other theoretical studies[16,17,34] for the C3−C2 and C4−O1 bonds. Thus, in d-I the length of the C3−C2 bond adjacent to the methylene group was found to be shorter than the length of the C3−C4 bond adjacent to the carbonyl group. Similarly, the

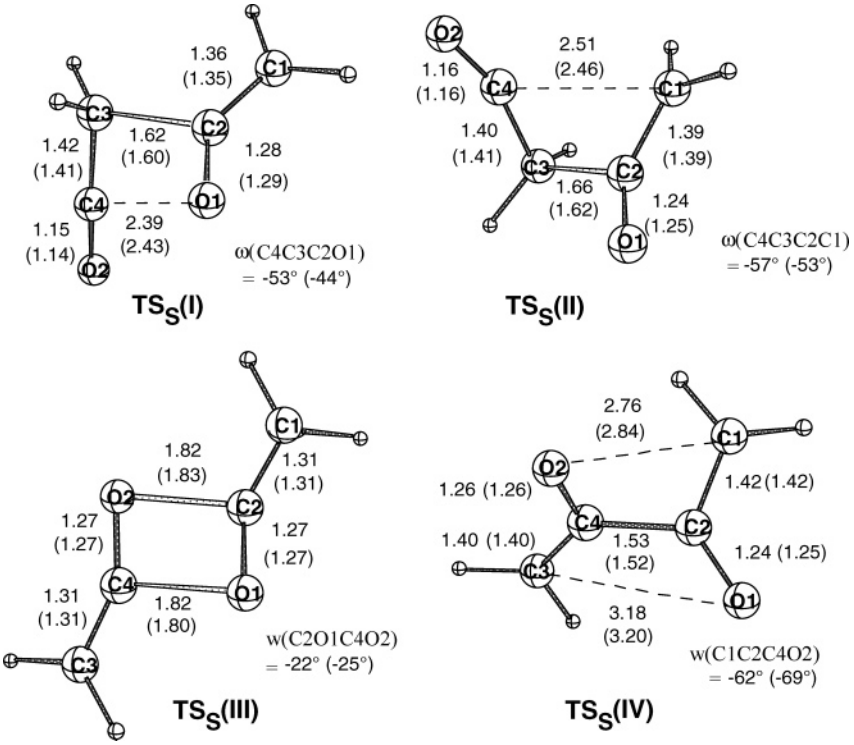

Figure 3. Some geometrical parameters for ketene dimerization transition states in liquid phase (bond lengths are given in angstroms): toluene solvent, no parentheses; acetone solvent, in parentheses.

CHART 2: Occupied and Virtual Orbitals on the C=C Double Bond of Ketene Monomer

CHART 3: Occupied and Virtual Orbitals on the CO Group of Ketene Monomer

length for the C4−O1 bond adjacent to the carbonyl group was found to be shorter than the length of the C2−O1 bond adjacent to the methylene group (Figure 1). These trends are in disagreement with the experimental molecular parameters obtained from electron diffraction.[35] The electron diffraction experiment predicted (assumed) the same length for the two different C−C and C−O bonds, respectively. X-ray diffraction data[36] for d-I show the two C−C bonds to be the same and longer than the theoretical estimates. On the other hand the two C−O bond lengths from X-ray diffraction follow the same trend as theory. However, the difference is much larger. Seidl and Schaefer[34] have previously assessed the differences between theory and the experimental molecular structures.

The discrepancies between the different available molecular structures for the d-I dimer can be assessed by comparing the corresponding values for the predicted rotational constants with those obtained directly from a microwave spectrum.[37] The rotational constants corresponding to theoretical and experimental molecular structures of the d-I dimer are compared in Table 2. The values corresponding to the structure obtained in this work show an absolute deviation of 56 MHz compared to the experimental values from the microwave spectrum. This absolute deviation for the d-I dimer structure found here is the smallest among the calculated deviations from the rotational constants based on both theoretical and experimental molecular structures. This suggests that the geometric parameters predicted at the PW86x+PBEc/DZP level of theory adequately represent the molecular structure for the d-I dimer. For the other dimers, there are no experimental geometric data available in the literature. However, the results obtained in this work are in good agreement with previous predictions at the MP2/6-31G(d)[16] and MP2/aug-cc-pVDZ[17] levels of theory (Figure 1). For the other dimers d-II to d-IV, the agreement between our structures and geometries optimized by other theoretical approaches is excellent (Figure 1).

Gas-Phase Transition States for the Dimerization Process. The optimized dimerization transition states in the gas phase are shown in Figure 2 as TS$_g$(I)−TS$_g$(IV). The corresponding transition states in the liquid state are shown as TS$_S$(I)−TS$_S$(IV) in Figure 3. All transition states were characterized by a frequency analysis and verified by IRC calculations. Both TS$_g$(I) and TS$_g$(II) are consistent with dimerization processes in which the formation of the first bond (represented by C2−C3) precedes the formation of the second bond, O1−C4 for d-I and C1−C4 for d-II. It should be noted that isomerization between d-I and d-II could take place via the two transition states TS$_g$(I) and TS$_g$(II) by a rotation around the C3−C2 bond. Such an isomerization was observed experimentally for the d-I type dimer of *p*-methoxyphenylketene by the reaction with potassium hydroxide in aqueous dioxane[38a] and for the d-II type dimer of the dimethylketene when heated with a trace of aluminum chloride.[38b] Previous structures for TS$_g$(I) and TS$_g$(II) due to Salzner and Bachrach[16] at the MP2/6-31G(d) level and by Rode and Dobrowolski[17] at the MP2/aug-cc-pVDZ level are in reasonable agreement with those found in the present work (Figure 2). The two studies also found TS$_g$(I) and TS$_g$(II) to be nonplanar.

A synchronous and coplanar approach in TS$_g$(I) and TS$_g$(II) would have resulted in a [$_\pi 2_s + _\pi 2_s$] symmetry forbidden cy-

TABLE 2: Rotational Constants for the d-I Dimer[a]

method	A	B	C	absolute deviation
microwave spectrum[37]	12 141.36 ± 0.04	2781.27 ± 0.01	2296.59 ± 0.01	
electron diffraction[35]	11 711 (−430)	2846 (65)	2323 (26)	521
X-ray crystallography[36]	11 757 (−387)	2736 (−45)	2250 (−47)	479
MP2/aug-cc-pVDZ[17]	12 053 (−88)	2716 (−65)	2249 (−47)	200
CISD/DZd[34]	12 289 (148)	2798 (17)	2313 (16)	181
CCSD/DZd[34]	12 051 (−90)	2747 (−34)	2270 (−27)	151
MP2/6-31G(d)[16]	12 044 (−97)	2777 (−4)	2290 (−6)	107
PW86x+PBEc/DZP	12 139 (2)	2749 (32)	2274 (22)	56

[a] Rotational constants are given in megahertz. Numbers in parentheses indicate the deviation from experimental microwave results. Rotational constants for the electron diffraction and X-ray structures were taken from ref 34.

CHART 4: Virtual and Occupied Orbitals Involved in the Formation of TS_g(I) and TS_g(II)

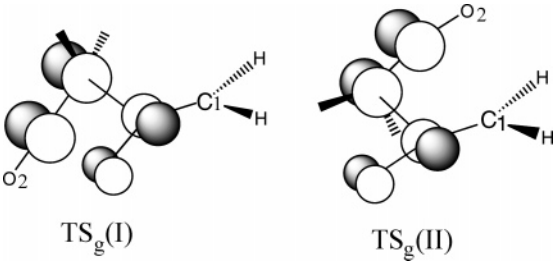

cloaddition.[39] By adopting instead a nonplanar asynchronous approach the initial part of the dimerization process in TS_g(I) and TS_g(II), leading to the formation of the C3−C2 bond, can be viewed as an allowed nucleophilic attack of C3, using the occupied π_{CC} orbital, on the carbonyl carbon *C*2 with the virtual π^*_{CO} orbital, Chart 4. In TS_g(I), the subsequent attack of O1 (with π_{CO}) on C4 (with π^*_{CC}) leading to the O1−C4 bond can take place without any further rearrangement as ω(C4,C3,C2,-O1) tends to zero. In TS_g(I), the second C4−C1 bond-making step must be accompanied by the rotation of the methylene group around the former C1═C2 double bond. It follows from Figures S4 and S5, where we depict the IRC of the two dimerization reactions leading to d-I and d-II, that the second rearrangement step involving O1−C4 or C4−C1 bond formation takes place without a second barrier. Thus, once TS_g(I) or TS_g-(II) has been reached, the energy decreases all the way down to the product. The two-step cycloaddition mechanism discussed here has also been observed in ketene addition to CH_2═CH_2, CH_2═O, and CpO_2Re═O by Deubel.[40] It is referred to as a nonplanar pseudopericyclic reaction.[17]

The formation of dimers d-III and d-IV has been studied to a lesser degree than the generation of d-I and d-II. We find that TS_g(III) corresponds to a synchronous cycloaddition in which the C2−O1−C4−O2 ring is slightly puckered with a dihedral angle of ω(C2,O1,C4,O2)= −22.4°. TS_g(III) is consistent with a thermally forbidden [$_\pi$2$_s$ + $_\pi$2$_s$] mechanism[39] where the bond formation involves the two (π_{CO}/π^*_{CO}) sets of orbitals on the CO groups (Chart 3). The formation of d-IV is, according to TS_g(IV), asynchronous. As in TS_g(I), the first step is C−C formation. However, in contrast to TS_g(I), where use was made of the occupied π_{CC} orbital and the virtual π^*_{CO} orbital (Chart 4), the process in TS_g(IV) involves the π_{CO} orbital on one monomer and π^*_{CO} on the other hand. After formation of the C4−C2 bond in TS_g(IV), the methylene group containing C1 has to rotate prior to formation of the C1−O1 bond. It is clear from Figures S6 and S7 where we display the IRC energy profile for the formation of d-III and d-IV that no intermediate (or second transition state) is located between TS_g(III), TS_g(IV), and the products d-III, d-IV.

On the basis of the semiempirical SINDO method, Jug et al.[13] concluded in 1978 that the reaction leading to the d-III dimer is asynchronous with an intermediate located between TS_g(III) and d-III. In 1988, Fu et al.[14] analyzed the dimerization reaction using HF/STO-3G. These authors concluded that TS_g-(III) is consistent with a thermally forbidden [$_\pi$2$_s$+$_\pi$2$_s$] mechanism.[39] Very recently, Rode and Dobrowolski[17] analyzed the mechanisms for the production of the d-III and d-IV dimers using MP2/aug-cc-pVDZ. They obtained a synchronous nonplanar quasi-formed ring for the geometry of TS d-III and a nonsynchronous planar structure with C_{2h} symmetry for the TS d-IV. These authors classified the reaction toward the d-III dimer as pericyclic and toward the d-IV dimer as pseudopericyclic according to the results of their AIM study. The geometry obtained in this work for TS_g(III) is in good agreement with the results by Rode and Dobrowolski.[17] We analyzed the synchronous planar TS_g(III) structure proposed by Fu et al.[14] and found that according to single-point calculations the planar TS structure is approximately 1.5 kcal mol^{-1} less stable than the nonplanar one at the MPW1K level. That suggests that TS_g-(III) is nonplanar but still synchronous and that the cycloaddition reaction toward the d-III dimer, as was suggested by Rode and Dobrowolski, might be classified as pericyclic.

Our structure for the TS d-IV is in disagreement with the planar structure proposed by Rode and Dobrowolski.[17] We carried out additional calculations enforcing the symmetry obtained for Rode and Dobrowolski. However, we could not find any transition state with C_{2h} symmetry for the TS d-IV at the PW86x+PBEc/DZP level. Additionally, we applied single-point calculations at the MPW1K level, obtaining a barrier of 111.12 kcal mol^{-1} for the TS d-IV of Rode and Dobrowolski. This barrier is much greater than the value of 65.2 kcal mol^{-1} obtained in this work for the TS d-IV at the same level of theory. This relative stabilization of the TS d-IV may be explained by the short distance in the C4−C2 formed bond. The results above suggest a reclassification of the reaction toward the d-IV dimer as nonplanar pseudopericyclic.

Liquid-Phase Transition States for the Dimerization Process. Solvation reduces the distance between C3 and C2 in TS_S(I) and TS_S(II) (Figure 3). In the case of TS d-I, that distance is reduced by 0.09 Å when the solvent is toluene and 0.11 Å when the solvent is acetone (Figures 3 and 4). For TS_S(II) the reduction is 0.07 Å in toluene and 0.11 Å in acetone. The changes are caused by solvation polarization of the C2−O1 bond, which makes the positive charge on C2 larger and facilitates nucleophilic attack by C3 in both TS_s(I) and TS_s(II). We shall shortly see that the C2−O1 bond polarization will lower the dimerization activation energy for d-I and d-II compared to the corresponding activation barriers in the gas phase. It follows in general from Table 3 that the Mayer bond orders[41] for the emerging bonds in TS_S(I) and TS_S(II) increase upon going from gas phase to liquid phase (Table 3). The changes in geometry and bond order for TS(IV) and especially TS(III) are smaller in going from gas phase to solution, as one

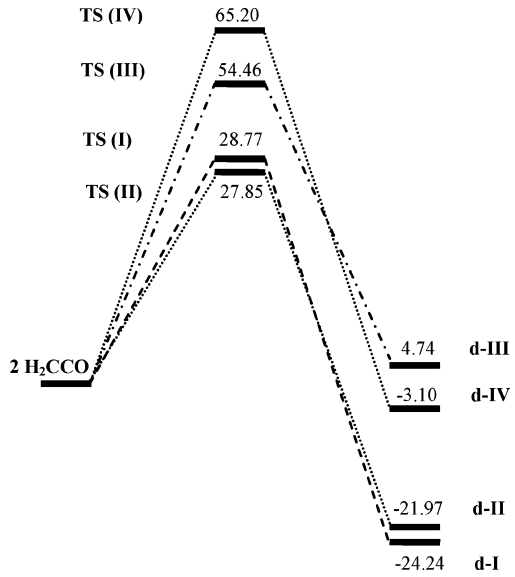

Figure 4. Relative enthalpies (1 atm and 298.15 K) for the ketene dimerization reaction according to the MPW1K/DZP//PW86x+PBEc/DZP level in kilocalories per mole. Zero point energy (ZPE) corrections are included.

TABLE 3: Bond Order for the Transition States[a]

		bond order		
structure	bond[b]	gas phase	toluene	acetone
TS(I)	C3−C2	0.680	0.766	0.783
TS(I)	O1−C4	0.203	0.236	0.235
TS(II)	C3−C2	0.665	0.721	0.758
TS(II)	C4−C1	0.255	0.270	0.300
TS(III)	C4−O1	0.455	0.448	0.471
TS(III)	C2−O2	0.456	0.450	0.448
TS(IV)	C4−C2	0.873	0.896	0.875
TS(IV)	O1−C3	0.345	0.233	0.253
TS(IV)	C1−O2	0.103	0.150	0.152

[a] Based on the Mayer methodology.[41] [b] See Figures 2 and 3 for labeling of atoms.

would expect for transition states with zero [TS(III)] or modest dipole moments.[42]

IRC calculations in both gas phase and solution showed that the ketene dimerization reactions for d-I, d-II, and d-IV proceed in two steps. The first is formation of a C−C bond leading to the transition state [TS_S(I), TS_S(II), and TS_S(IV)] and an activation barrier. The next step is the formation of a C−O bond for d-I and d-IV and a C−C bond for d-II. This step proceeds without barrier. On the other hand, d-III is formed in a concerted fashion where the two CO bonds emerge at the same time in TS_S(III). More detailed information can be found in Figures S1−S7 of the Supporting Information.

Energies in Gas Phase. It has been reported that the experimental activation energy[12] and the heat of reaction[43] for formation of the ketene dimer (d-I) are 31 kcal/mol and −22.6 kcal/mol, respectively. Further on, d-I was found[12] experimentally to be less stable than d-II by 1 kcal/mol in the gas phase. Experimental activation parameters in the gas phase have not been reported for the dimerization to d-II.

We have carried out single-point calculations with different meta and hybrid functionals[44−46] available in the ADF package based on the optimized structures at the PW86x+PBEc/DZP level in order to obtain the functional that best fits the reported experimental values. The complete list of the 58 studied functionals can be found in Table S8 of the Supporting Information. We find the best performance for the MPW1K[45] functional. Thus, MPW1K was selected to study the ketene dimerization reaction in both gas and liquid phase. The B1PW91[45b,47] and MPW1PW[45b,48] functionals, which belong to the same family as MPW1K, had nearly the same performance (Table S8).

Table 4 displays gas-phase enthalpies and Gibbs energies of formation for the ketene dimerization reaction at 298.15 K and 1 atm, based on the energies calculated at the MPW1K/DZP//PW86x+PBEc/DZP level. Both d-I and d-II are stable on the Gibbs energy surface with d-I favored over d-II by 2 kcal/mol. On the other hand, both d-III and d-IV have positive Gibbs energies of formation and are thus not likely to form in noticeable concentrations from ketene dimerization. In terms of enthalpy, d-I is again favored over d-II by 2 kcal/mol, whereas the formation of d-III and d-IV is highly endothermic. Kinetically the enthalpy of activation is 2 kcal/mol higher for the thermodynamically favored product d-I. This difference is cut to 0.5 kcal/mol on the Gibbs energy surface. The high barriers for d-III and d-IV make d-III and d-IV unlikely dimerization products (Figure 4).

In what is likely the most extensive DFT study on ketene dimerization to date, we find that d-II is the kinetically favored product although d-I is more stable than d-II. However, the calculated differences in activation and formation energies between the two species are too close to the error margin of our theoretical method to make our findings conclusive. We note that most of the functionals examined here find d-I to be more stable than d-II in the gas phase, although experiment[12] favors d-II over d-I with 1 kcal/mol. It is important to mention that theoretical and experimental results for the heat of formation for ketene compounds typically have been in disagreement.[49]

There have been several ab initio studies on ketene dimerization in the gas phase.[13−18] Most recently, Rode and Dobrowolski[17] found from high-level G3 calculations that d-I is more stable than d-II by 2 kcal/mol, whereas the dimerization barrier for d-I is lower than for d-II by 0.4 kcal. As stated by the authors, the calculated differences are too small to make definitive conclusions. On the other hand, it would also be interesting to revisit the combustion data used[12] experimentally to reassess the energy difference between d-I and d-II and to establish the dimerization barrier experimentally for d-II.

Up to now, our discussion of the energetics for the dimerization process has been restricted to the gas phase. However, most dimerization reactions have been carried out in solution.[10−12,50] As a consequence, we shall now include solvation into our simulation.

Energies in Liquid Phase. Table 4 displays enthalpies and Gibbs energies of formation for the ketene dimerization reaction based on the energies calculated at the MPW1K/DZP//PW86x+PBEc/DZP level in toluene and acetone.

It follows from Table 4 that the dimerization becomes energetically more favorable in solution compared to the gas phase. On the enthalpic surface this stabilization comes from a favorable interaction between the dimer dipole and the solvent, especially for d-I, d-II, and d-IV. In fact, for d-I, d-II, and d-IV, the dimer dipole is enhanced by increasing solvent polarity in order to optimize this interaction. On the Gibbs energy surface, a further stabilization is obtained compared to the gas phase by an increase in the dimerization entropy (Table 4 and Figure 5; eqs 2 and 3). We note that, even in a polar solvent, d-III and d-IV are unlikely to form on thermodynamic grounds (Table 4). Further, d-I remains more stable than d-II in terms of both

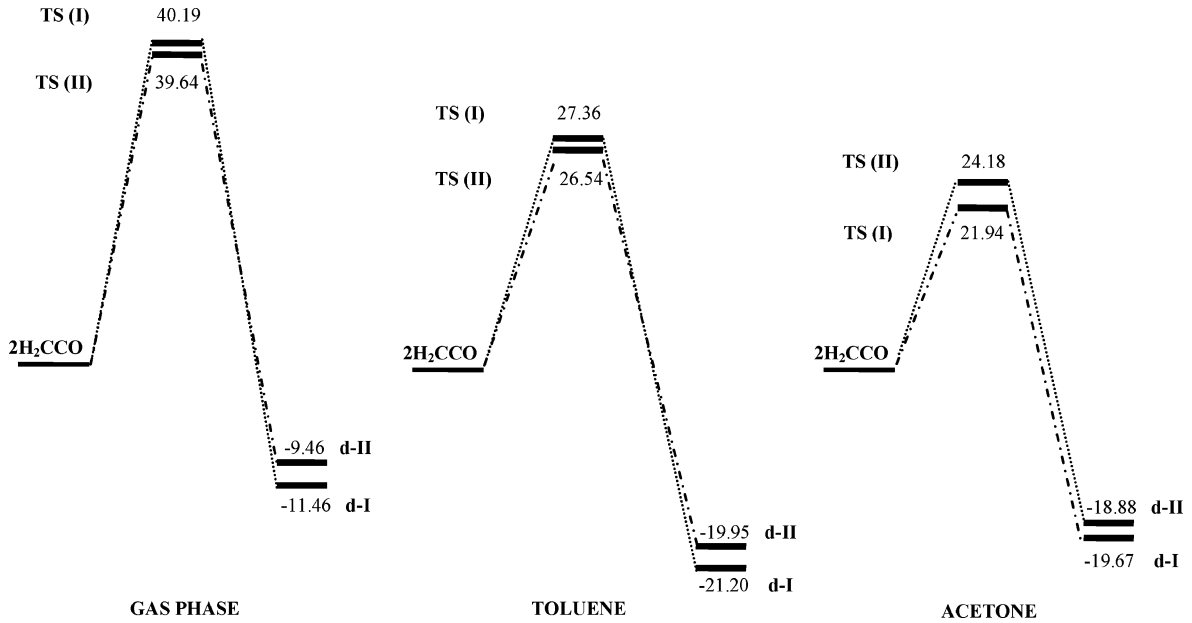

Figure 5. Gibbs energies for the production of the d-I and d-II dimers at the PW1K/DZP//PW86x+PBEc/DZP level in kilocalories per mole. $T = 298.15$ K, $P = 1$ atm.

TABLE 4: Energetics for the Forward Reactions[a,b]

	gas phase			toluene solution[c]			acetone solution[c]		
	ΔH	ΔS	ΔG	ΔH	ΔS	ΔG	ΔH	ΔS	ΔG
TS(I)	28.77 (31)	−38.32	40.19	20.76	−22.13	27.36 (22.15)	13.83 (10)	−27.20 (−38)	21.94 (21.17)
TS(II)	27.85	−39.53	39.64	19.92	−22.20	26.54	15.83	−28.01	24.18
TS(III)	55.88	−37.97	67.20	52.61	−21.12	58.91	52.92	−26.49	60.81
TS(IV)	66.33	−40.64	78.45	61.34	−25.90	69.06	57.38	−26.15	65.17
d-I	−24.24 (−22.67)	−42.85	−11.46	−28.39	−24.10	−21.20	−28.62	−30.02	−19.67
d-II	−21.97	−41.95	−9.46	−26.77	−22.87	−19.95	−27.47	−28.80	−18.88
d-III	4.74	−42.71	17.48	3.10	−23.97	10.25	3.49	−29.91	12.41
d-IV	−3.10	−42.00	9.42	−6.66	−23.60	0.38	−6.53	−29.49	2.26

[a] At 298.15 K and 1 atm, calculated at the MPW1K/DZP//PW86x+PBEc/DZP level. [b] Experimental data are shown in parentheses (gas phase from ref 12 and liquid phase from ref 10). ΔS values are given in calories per mole per kelvin. ΔH and ΔG values are given in kilocalories per mole. [c] Temperatures of experiments (ref 10) for toluene and acetone were 273.15 and 293.15 K, respectively.

TABLE 5: Dipole Moments[a] for the Transition States in Gas and Liquid Phase

	gas phase	toluene	acetone
TS(I)	4.331	5.715	7.532
TS(II)	3.777	5.023	6.086
TS(III)	0.900	1.080	1.070
TS(IV)	2.733	3.275	4.392
monomer	1.462	1.734	2.000

[a] Dipole moments are given in Debyes.

ΔH and ΔG. However, the gap is reduced from 2 kcal/mol in the gas phase to 1 kcal/mol in acetone (Table 4 and Figure 5).

Kinetically, all enthalpy barriers are lowered in solution by a solvent-induced polarization, especially of $TS_S(I)$, $TS_S(II)$, and $TS_S(IV)$ (Table 5). The Gibbs energy barriers are lowered further by an increase in the activation entropies through eqs 2 and 3, when the solvents are acetone and toluene, respectively (see Figure 5 and Table 4). We note that $TS_S(I)$ is stabilized relative to $TS_S(II)$ by solvent effect, so that the rate of formation of d-I exceeds that of d-II in the polar solvent acetone, whereas the rate of formation of d-II still is larger in gas phase and toluene. According to this result, the experimental detection of the d-I dimer in toluene[10] may be explained by isomerization of the first formed d-II dimer. The barriers of activation for d-III and d-IV are too high even in acetone for any of these species to form.

The calculated value for the Gibbs energy barrier of $TS_S(I)$ in toluene is overestimated by 5.2 kcal/mol compared to experiment[10] (Table 4). The calculated value of 21.94 kcal mol^{-1} for the Gibbs energy barrier of $TS_S(I)$ in acetone is in good agreement with the experimental estimate[10] of 21.17 kcal mol^{-1}. However, the activation energy and the entropy differ by 4 kcal mol^{-1} and 11 cal mol^{-1} K^{-1}, respectively, from the experimental values (Table 4). It is quite common that Gibbs energy changes in solution are easier to determine than the individual enthalpic and entropic components, as solvent systems can undergo enthalpy−entropy compensations[51] that are difficult to describe with a simple continuum model.

The results in acetone indicate that the d-I dimer is favored both kinetically and thermodynamically over the other dimers. However, the d-II dimer may be produced in a small amount during the ketene dimerization in acetone solvent. According to the values obtained in this work for the Gibbs energy barriers in acetone, the d-II dimer is produced in a yield of approximately

3%. This prediction is in excellent agreement with the results of Tenud et al.,[50] who reported that a small amount of the symmetrical d-II dimer, 1,3-cyclobutanedione, was produced in a yield between 4% and 5% in acetone.

Conclusions

We have carried out the first extensive theoretical comparison of ketene dimerization in gas phase and in solution. The four dimerization products considered are diketene (d-I), 1,3-cyclobutanedione (d-II), 2,4-dimethylene-1,3-dioxetane (d-III), and 2-methyleneoxetan-3-one (d-IV) (Chart 1). It was found in both gas phase and solution that all four dimerization processes involve a single transition state without intermediates. For d-I, d-II, and d-IV, dimerization is asynchronous with the formation of one bond preceding formation of the other. On the other hand, dimerization leading to d-III is synchronous with both bonds forming at the same time. The ketene dimerizations toward the d-I, d-II, and d-IV dimers might be classified as nonplanar pseudopericyclic reactions. The ketene dimerization process leading to the d-III dimer is, on the other hand, a pericyclic reaction with a nonplanar but still synchronous transition state.

Solvation makes dimerization more favorable in solution than in gas phase as the products, especially d-I, d-II, and d-IV, are stabilized by interactions between the solute dipoles and the solvent. Similar interactions in the transition states TS_S(I), TS_S-(II), and TS_S(IV) help lower the activation enthalpies compared to the gas phase. An increase in the entropy of dimerization and activation in solution compared to gas phase help further ease the formation of the dimers kinetically as well as thermodynamically in solution. The species d-III and d-IV have higher energies and dimerization barriers than d-I and d-II. As a consequence, d-III and d-IV are unlikely products from ketene dimerization in gas phase as well as in solution.

The species d-I was calculated to be more stable than d-II in gas phase as well as solution. However, the calculated margin is reduced from 2 kcal/mol in gas phase to 1 kcal/mol in acetone. On the other hand, whereas d-II is calculated to have the lowest dimerization barrier in gas phase and modestly nonpolar solvents, d-I has the lowest barrier in polar solvents such as acetone. Our results are in good agreement with experiments carried out in solvents. However, in gas-phase experiments d-II is more stable than d-I, in contrast to our calculation as well as other recent studies.

Acknowledgment. G.M. and R.M. acknowledge the financial support of Universidad Industrial de Santander, UIS (Colombia), and Instituto Colombiano para el Desarrollo de la Ciencia y la Tecnología Francisco José de Caldas, programa Apoyo a la Comunidad Científica Nacional por Medio de Doctorados Nacionales, COLCIENCIAS (Colombia). T.Z. thanks the Canadian government for a Canada Research Chair.

Supporting Information Available: Nine tables showing PW86x+PBEc/DZP calculated geometries, dipole moments, and atomic charges for the dimers and their corresponding TS structures in gas and liquid phase;− single-point calculations for the ketene dimerization toward the d-I dimer using different meta functionals and hybrid functionals; and thermochemical properties for the dimers and their corresponding transition states at the MPW1K/DZP level; and seven figures showing linear transit search profiles for the ketene dimerization reactions in gas phase at the PW86x+PBEc/DZP level −and IRC profiles for the ketene dimerization toward the different studied dimers.− This information is available free of charge via the Internet at http://pubs.acs.org.

References and Notes

(1) Ulrich, H. *Cycloaddition Reactions of Heterocumulenes*; Academic Press: New York and London. 1967.

(2) (a) Holden, K. G. *Chemistry and Biology of β-Lactam Antibiotics*, Vol. 2; Morin, R. B., Gorman, M., Eds.; Academic: New York, 1982. (b) Palomo, C.; Aizpurua, J. M.; Iñaki, G.; Oiarbide, M. Asymmetric Synthesis of β-Lactams by Staudinger Ketene-Imine Cycloaddition Reaction. *Eur. J. Org. Chem.* **1999**, *12*, 3223−3235. (c) Tidwell, T. T. *Ketenes*; Wiley: New York, 1995 and references therein. (d) Collins, P. W.; Djuric, S. W. Synthesis of Therapeutically Useful Prostaglandin and Prostaciclyn Analogs. *Chem. Rev.* **1993**, *93*, 1533−1564. (e) Foland, L. D.; Karlsson, J. O.; Perri, S. T.; Schwabe, R.; Xu, S. L.; Patil, S.; Moore, H. W. Rearrangement of 4-Alkynylcyclobutenones. A New Synthesis of 1,4-Benzoquinones. *J. Am. Chem. Soc.* **1984**, *111*, 975−989. (f) Li, C. Y.; Wang, X. B.; Sun, X. L.; Tang, Y.; Zheng, J. C.: Xu, Z. H.; Zhou, Y. G.; Dai, L. X. Iron Porphyrin-Catalized Olefination of Ketenes with Diazoacetate for the Enantioselective Synthesis of Allenes. *J. Am. Chem. Soc.* **2007**, *129*, 1494−1495. (g) Paull, D. H.; Alden-Danforth, E.; Wolfer, J.; Dogo-Isonagie, C.; Abraham, C. J.; Lectka, T. An Asymmetric, Bifunctional Catalytic Approach to Non-Natural α-Amino Acid Derivatives. *J. Org. Chem.* **2007**, *72*, 5380−5382. (h) Ma, G.; Nguyen, H.; Romo, D. Concise Total Synthesis of (±)-Salinosporamide A, (±)-Cinnabaramide A, and Derivatives via a Bis-cyclization Process: Implications for a Biosynthetic Pathway? *Org. Lett.* **2007**, *9*, 2143−2146.

(3) (a) Chick, F; Wilsmore, N. T. M. Acetylketen: a Polymeride of Keten. *J. Chem. Soc.* **1908**, 946−950. (b) Staudinger, H.; Klever, H. W. Über Ketene. 6. Mitteilung: Keten. *Ber. Dtsch. Chem. Ges.* **1908**, *41*, 594−600.

(4) Hyatt, J. A.; Raynolds, P. W. Ketene Cycloadditions. *Org. React*. **1994**, *45*, 160−246.

(5) Clemens, R. J. Diketene. *Chem. Rev.* **1986**, *86*, 241−318.

(6) Scholl, T.; Jackson, B. Process for the Production of Squaric Acid. U.S. Patent 5,130,492, 1992.

(7) Naka, K.; Uemura, T; Chujo, Y. Synthesis of Polymers Having 1,3-Cyclobutanedione Unit in the Main Chain by Cycloaddition Polymerization of Bisketene. *Polym. Bull.* **1999**, *42*, 367−372.

(8) (a) Kato, E.; Osawa, S. Color Image Forming Method. U.S. Patent 5,582,941, 1996. (b) Nakazawa, Y.; Ishii, K.; Kato, E. Method of Lithographic Printing. U.S. Patent 6,862,992, 2005.

(9) Dejaegher, Y.; Kuz'menok, N. M.; Zvonok, A. M.; De Kimpe, N. The Chemistry of Azetidin-3-ones, Oxetan-3-ones, and Thietan-3-ones. *Chem. Rev.* **2002**, *102*, 29−60.

(10) Rice, F. O.; Greenberg, J. Ketene II. Rate of Polymerization. *J. Am. Chem. Soc*. **1934**, *56*, 2132−2134.

(11) (a) Williams, J. W.; Krynitsky, J. A. Ketene Dimer. *Org. Synth*. **1955**, *3*, 508. (b) Sturzenegger, A. Preparation of Diketene. U.S. Patent 2,802,872, 1957. (c) Lacey, R. N. Dimerisation of Ketene in Medium of Diketene and Acetic Anhydride. U.S. Patent 2,848,496, 1958. (d) Zima, H. Stabilized Diketene and Method for its Production. U.S. Patent 3,271,420, 1966. (e) Bergmin, R.; Quittmann, W.; Stoffel, J. Process for the Reduction of the Polymer Portion in the Dimerization of Ketene. U.S. Patent 4,999,-438, 1990.

(12) Chickos, J. S.; Sherwood, D. E., Jr.; Jug, K. Mechanism of Thermolysis of Diketene in the Gas Phase. *J. Org. Chem*. **1978**, *43*, 1146−1150.

(13) Jug, K.; Dwivedi, C. P. D.; Chickos, J. S. Reaction Pathways for Various Ketene Dimers. *Theor. Chim. Acta* **1978**, *49*, 249−257.

(14) Fu, X. Y.; Decai, F.; Yanbo, D. Theoretical Studies on the Reaction Mechanism of Ketene Dimerization Reactions. *J. Mol. Struct. (THEOCHEM)* **1988**, *167*, 349−358.

(15) Seidl, E. T.; Schaefer, H. F., III. Theoretical Investigations on the Dimerization of Ketenes: Does the 2S + 2A Cycloaddition Reaction Exist? *J. Am. Chem. Soc*. **1991**, *113*, 5195−5200.

(16) Salzner, U.; Bachrach, M. S. Ab Initio Studies of the Dimerization of Ketene and Phosphaketene. *J. Am. Chem. Soc*. **1994**, *116*, 6850−6855.

(17) Rode, J. R.; Dobrowolski, J. Cz. Reaction Paths of the [2 + 2] Cycloaddition of X=C=Y Molecules (X, Y = S or O or CH_2). Ab Initio Study. *J. Phys. Chem. A* **2006**, *110*, 207−218.

(18) Kelly, E.; Seth, M.; Ziegler, T. Calculation of Free Energy Profiles for Elementary Bimolecular Reactions by ab Initio Molecular Dynamics: Sampling Methods and Thermostat Considerations. *J. Phys. Chem. A* **2004**, *108*, 2167−2180.

(19) Huisgen, R.; Otto, P. The Mechanism of Dimerization of Dimethylketene. *J. Am. Chem. Soc*. **1968**, *90*, 5342−5343.

(20) Rice, F. O.; Roberts, R. The Structure of Diketene. *J. Am. Chem. Soc*. **1943**, *65*, 1677−1681.

(21) Perdew, J. P. Density-Functional Approximation for the Correlation Energy of the Inhomogeneous Electron Gas. *Phys. Rev. B* **1986**, *33*, 8822−8824.

(22) Perdew, J. P.; Burke, K.; Ernzerhof, M. Generalized Gradient Approximation Made Simple. *Phys. Rev. Lett*. **1996**, *77*, 3865−3868.

(23) Baerends, E. J.; Ellis, D. E.; Ros, P. Self-Consistent Molecular Hartree-Fock-Slater Calculations I. The Computational Procedure. *Chem. Phys.* **1973**, *2*, 41−51.

(24) Krijn, J. G.; Baerends, E. J. *Fit Functions in the HFS-Method*; Internal Report (in Dutch); Vrije Universiteit Amsterdam: Amsterdam, The Netherlands, 1984.

(25) McQuarrie, D. A. *Statistical Thermodynamics*; Harper: New York, 1973.

(26) Fukui, K. The Path of Chemical Reactions−the IRC Approach. *Acc. Chem. Res.* **1981**, *14*, 363−375.

(27) Te Velde, G.; Bickelhaupt, F. M.; Baerends, E. J.; van Gisbergen, S.; Guerra, C. F.; Snijders, J. G.; Ziegler, T. Chemistry with ADF. *J. Comput. Chem*. **2001**, *22*, 931−967.

(28) Klamt, A.; Schuurmann, G. COSMO: A New Approach to Dielectric Screening in Solvents with Explicit Expressions for the Screening Energy and its Gradient. *J. Chem. Soc., Perkin. Trans*. **1993**, *2*, 799−805.

(29) Pye, C. C.; Ziegler, T. An Implementation of the Conductor-Like Screening Model of Solvation within the Amsterdam Density Functional Package. *Theor. Chem. Acc*. **1999**, *101*, 396−408.

(30) Wertz, D. H. Relationship between the Gas-Phase Entropies of Molecules and their Entropies of Solvation in Water and 1-Octanol. *J. Am. Chem. Soc*. **1980**, *102*, 5316−5322.

(31) Cooper, J.; Ziegler, T. A Density Functional Study of S_N2 Substitution at Square-Planar Platinum(II) Complexes. *Inorg. Chem*. **2002**, *41*, 6614−6622.

(32) Lide, D. R., Ed. *CRC Handbook of Chemistry and Physics*, 86th ed.; CRC Press: Boca Raton, FL, 2006 (http://www.hbcpnetbase.com/).

(33) National Institute of Standards and Technology. *Computational Chemistry Comparison and Benchmark DataBase* (http://srdata.nist.gov/cccbdb/).

(34) Seidl, E. T.; Schaefer, H. F. Molecular Structure of Diketene: A Discrepancy between Theory and Experiments? *J. Phys. Chem*. **1992**, *96*, 657−661.

(35) Bregman, J.; Bauer, S. H. An Electron Diffraction Study of Ketene Dimer, Methylketene Dimer and β-Propiolactone. *J. Am. Chem. Soc*. **1955**, *77*, 1955−1965.

(36) Kay, M. I.; Katz, L. A Refinement of the Crystal Structure of Ketene Dimer. *Acta Crystallogr*. **1958**, *11*, 897−898.

(37) Mönnig, F.; Dreizler, H.; Rudolph, H. D. *Z. Naturforsch. A* **1967**, *22*, 1471−1473.

(38) (a) Farnum, D. G.; Johnson, J. R.; Hess, R. E.; Marshall, T. B.; Webster, B. Aldoketene Dimers and Trimers From Acid Chlorides. A Synthesis of Substituted 3-Hydroxycyclobutenones. *J. Am. Chem. Soc*. **1965**, *87*, 5191−5197. (b) Hasek, R H.; Clark, R. D.; Elam, E. U.; Martin, J. C. The Chemistry of Dimethylketene Dimer. IV. The Polyester and β-Lactone Dimer of Dimethylketene. *J. Org. Chem.* **1962**, *27*, 60−64.

(39) Woodward, R. B.; Hoffmann, R. The Conservation of Orbital Symmetry. *Angew. Chem., Int. Ed. Engl.* **1969**, *8*, 781−932.

(40) Deubel, D. V. Transition States for the [2+2] Addition of CH_2=CH_2, CH_2=O, and [M]=O Across the C=C Double Bond of Ketene: Electronic Structure and Energy Decomposition. *J. Phys. Chem. A* **2002**, *106*, 431−437.

(41) (a) Mayer, I. Charge, Bond Order and Valence in the Ab Initio SCF Theory. *Chem. Phys. Lett*. **1983**, *97*, 270−274. (b) Mayer, I. Comments on the Quantum Theory of Valence and Bonding: Choosing between Alternative Definitions. *Chem. Phys. Lett.* **1984**, *110*, 440−444.

(42) Pross, A. *Theoretical and Physical Principles of Organic Reactivity*. John Wiley & Sons, Inc.: New York, 1995.

(43) Mansson, M; Nakase, Y.; Sunner, S. The Enthalpies of Combustion and Formation of Diketene. *Acta Chem. Scand*. **1968**, *22*, 171−174.

(44) Xu, X.; Goddard, W. A., III. From the Cover: The X3LYP Extended Density Functional for Accurate Descriptions of Nonbond Interactions, Spin States, and Thermochemical Properties. *Proc. Natl. Acad. Sci. U.S.A.* **2004**, *101*, 2673−2677.

(45) (a) Lynch, B. J.; Fast, P. L.; Harris, M.; Truhlar, D. G. Adiabatic Connection for Kinetics. *J. Phys. Chem. A* **2000**, *104*, 4811−4815. (b) Exact exchange based on Watson, M. A.; Handy, N. C.; Cohen, A. J. Density Functional Calculations, Using Slater Basis Sets, with Exact Exchange. *J. Chem. Phys*. **2003**, *119*, 6475−6481.

(46) (a) Perdew, J. P.; Ernzerhof, M.; Burke, K. Rationale for Mixing Exact Exchange with Density Functional Approximations. *J. Chem. Phys.* **1996**, *105*, 9982−9985. (b) Ernzerhof, M.; Scuseria, G. Assessment of the Perdew−Burke−Ernzerhof Exchange-Correlation Functional. *J. Chem. Phys.* **1999**, *110*, 5029−5036. (c) Adamo, C.; Barone, V. Toward Reliable Density Functional Methods without Adjustable Parameters: The PBE0 Model. *J. Chem. Phys.* **1999**, *110*, 6158−6170.

(47) Adamo, C.; Barone, V. Toward Reliable Adiabatic Connection Models Free from Adjustable Parameters. *Chem. Phys. Lett*. **1997**, *274*, 242−250.

(48) Adamo, C.; Barone, V. Exchange Functionals with Improved Long-Range Behavior and Adiabatic Connection Methods without Adjustable Parameters: The *m*PW and *m*PW1PW Models. *J. Chem. Phys.* **1998**, *108*, 664−675.

(49) (a) Nguyen, M. T.; Nguyen, H. M. T. On the Heats of Formation of Methylketene, Dimethylketene and Related Cations. *Chem. Phys. Lett.* **1999**, *300*, 346−350. (b) Traeger, J. C. Neutral and Cationic Heats of Formation for Ketene, Methylketene, and Dimethylketene. *Int. J. Mass Spectrom.* **2000**, *194*, 261−267. (c) Sumathi, R.; Green, W. H., Jr. Thermodynamic Properties of Ketenes: Group Additivity Values from Quantum Chemical Calculations. *J. Phys. Chem. A* **2002**, *106*, 7937−7949.

(50) Tenud, L.; Weilenmann, M.; Dallwigk, E. 1,3-Cyclobutanodion-derivate aus Keten. *Helv. Chim. Acta* **1977**, *60*, 975−977.

(51) (a) Yu, H. A.; Karplus, M. A Thermodynamic Analysis of Solvation. *J. Chem. Phys*. **1988**, *89*, 2366−2379. (b) Williams, D. H.; Westwell, M. S. Aspects of Weak Interactions. *Chem. Soc. Rev.* **1998**, *27*, 57−63. (c) Liu, L.; Guo, Q. X. Isokinetic Relationship, Isoequilibrium Relationship, and Enthalpy−Entropy Compensation. *Chem. Rev.* **2001**, *11*, 673−695.